Neuron
Article

Extracellular Engrailed Participates in the Topographic Guidance of Retinal Axons In Vivo

Andrea Wizenmann,[1,2,7,9] Isabelle Brunet,[3,7,10] Joyce S.Y. Lam,[4,7] Laure Sonnier,[3,7] Marine Beurdeley,[3] Konstantinos Zarbalis,[1,2,11] Daniela Weisenhorn-Vogt,[1,2] Christine Weinl,[4,8] Asha Dwivedy,[4] Alain Joliot,[6] Wolfgang Wurst,[1,2,5] Christine Holt,[4,*] and Alain Prochiantz[3,*]

[1]Institute of Developmental Genetics, Helmholtz Zentrum Munich, Ingolstädter Landstrasse 1, 89675 Neuherberg, Germany
[2]MPI of Psychiatry, Kraepelinstrasse 1-10, 8004 Munich, Germany
[3]Group "Development and Neuropharmacology" (Equipe FRM), UMR 8542 CNRS-ENS-CDF, Collège de France, 11 place M. Berthelot, 75231 Paris, Cedex 05, France
[4]Department of Physiology, Development and Neurosciences, University of Cambridge, Downing Street, Cambridge CB2 3DY, UK
[5]Department of Developmental Genetics, German Centre of Neurodegenerative Diseases, Technical University Munich, Munich, Germany
[6]Group "Cell Biology of Homeoproteins," UMR 8542 CNRS-ENS-CDF, Collège de France, 11 place M. Berthelot, 75231 Paris, Cedex 05, France
[7]These authors contributed equally to this work
[8]Present address: Institute for Cell Biology, Department of Molecular Biology, University of Tuebingen, Auf der Morgenstelle 15, D-72076 Tuebingen, Germany
[9]Present address: Institut of Anatomy, Department of Experimental Embryology, University of Tuebingen, Oesterbergstrasse 3, D-72074 Tuebingen, Germany
[10]Present address: College de France, Inserm U833, 11 Place Marcelin Berthelot, F-75005 Paris, France
[11]Present address: University of California, Davis Medical Center, Department of Pathology, Institute for Pediatric Regenerative Medicine, Shriners Hospitals for Children, Northern California, 2425 Stockton Boulevard, Sacramento, CA 95817, USA
*Correspondence: ceh@mole.biol.cam.ac.uk (C.H.), alain.prochiantz@ens.fr (A.P.)
DOI 10.1016/j.neuron.2009.09.018

SUMMARY

Engrailed transcription factors regulate the expression of guidance cues that pattern retinal axon terminals in the dorsal midbrain. They also act directly to guide axon growth in vitro. We show here that an extracellular En gradient exists in the tectum along the anterior-posterior axis. Neutralizing extracellular Engrailed in vivo with antibodies expressed in the tectum causes temporal axons to map aberrantly to the posterior tectum in chick and *Xenopus*. Furthermore, posterior membranes from wild-type tecta incubated with anti-Engrailed antibodies or posterior membranes from Engrailed-1 knockout mice exhibit diminished repulsive activity for temporal axons. Since EphrinAs play a major role in anterior-posterior mapping, we tested whether Engrailed cooperates with EphrinA5 in vitro. We find that Engrailed restores full repulsion to axons given subthreshold doses of EphrinA5. Collectively, our results indicate that extracellular Engrailed contributes to retinotectal mapping in vivo by modulating the sensitivity of growth cones to EphrinA.

INTRODUCTION

Over 40 years ago, Sperry (Sperry, 1963) proposed that two orthogonal gradients in the retina give each retinal ganglion cell (RGC) a positional identity that could match up with gradients in the superior colliculus (SC) in mammals or optic tectum (Tec) in birds and amphibia. Ephrin ligands and their Eph receptors, expressed in complementary gradients in the retina and tectum, have been identified as key mediators in retinotectal mapping (Cheng et al., 1995; Drescher et al., 1995; Feldheim et al., 2004; Flanagan, 2006; Frisen et al., 1998; Mann et al., 2002; McLaughlin and O'Leary, 2005; O'Leary and Nakagawa, 2002). Along the anterior-posterior (A-P) axis, EphrinA2/A5 are expressed in a high-posterior to low-anterior gradient in the Tec/SC and repel retinal axons that express EphA3 receptor in a high-temporal to low-nasal gradient (Cheng et al., 1995; Drescher et al., 1995). In the EphrinA2/A5 double and EphrinA2/A3/A5 triple knockouts (Feldheim et al., 2000; Pfeiffenberger et al., 2006), the retinotectal map is highly abnormal; however, a small degree of A-P order still remains, indicating that additional mapping molecules exist. Indeed, adhesion molecule L1 (Buhusi et al., 2008; Schmid and Maness, 2008) and Semaphorin3F (Claudepierre et al., 2008) can modulate A-P retinotectal map formation, and further molecular pathways may exist.

During midbrain development, the earliest proteins expressed in a high-posterior to low-anterior gradient are the homeodomain transcription factors Engrailed1 (En1) (Wurst et al., 1994) and Engrailed2 (En2) (Hemmati-Brivanlou et al., 1991 ; Joyner and Hanks, 1991). En1 and En2 are partially redundant as shown by normal midbrain phenotype in the *En2* knockout or the knockin of *En2* into *En1* (Hanks et al., 1995; Joyner and Hanks, 1991). When En1 or En2 (collectively, Engrailed or En1/2) are ectopically expressed in the tectum, temporal axons avoid these

areas, whereas nasal axons tend to terminate in them (Friedman and O'Leary, 1996; Itasaki and Nakamura, 1996). EphrinA upregulation at ectopic En1/2 sites supports the view that En1/2 control rostrocaudal patterning by regulating the graded expression of cell surface molecules (Logan et al., 1996; Shigetani et al., 1997). Attraction of nasal axons to the ectopic En1/2 sites, once puzzling given the in vitro evidence that EphrinA repels axons, could be explained by more recent studies showing that EphrinA promotes axon growth in a concentration-dependent manner in vitro (Hansen et al., 2004; Weinl et al., 2005). Other possibilities include unidentified attractants and/or Engrailed itself playing a direct role in attracting nasal axons.

The possibility that Engrailed itself plays a direct role is suggested by studies showing that an external gradient of soluble En2 attracts nasal axons and repels temporal axons (Brunet et al., 2005). These findings prompted us to test whether En plays an extracellular role in map formation. Furthermore, Engrailed proteins can be secreted and internalized in vitro and are associated with vesicles in the SC (Joliot and Prochiantz, 2004; Joliot et al., 1997). Thus, as shown for Pax6 in the eye anlagen (Lesaffre et al., 2007) and Otx2 in the visual cortex (Sugiyama et al., 2008), En1/2 could have non-cell-autonomous activities in the optic tectum. The data presented support this hypothesis and indicate that extracellular Engrailed contributes to map formation possibly via a mechanism that adjusts the sensitivity of axons to EphrinAs.

RESULTS

Extracellular Membrane-Tethered Engrailed in the Tectum

We first asked whether En1/2 associate with tectal cell membranes. Nuclear and membrane fractions were prepared from E9 chick tecta, and En1/2 were found in the two fractions (Figure 1A). The absence of cross-contamination between the two fractions was verified using the nuclear marker RNA polymerase II (Pol-II) and the membrane marker GM130 (Nakamura et al., 1997). By separating the most anterior (A) and posterior (P) domains of the tectum, we found that the low/anterior-high/posterior Engrailed nuclear gradient is preserved in the membranes (Figure 1A). The equal presence of β-actin and of a contaminant HSC70 extracellular isoform migrating between En1 and En2 indicates that similar amounts of proteins were loaded on A and P lanes.

To investigate whether membranous En1/2 are localized outside of the cells, extracellular proteins from E9 anterior (A), median (M), and posterior (P) domains of chick tectum in flat-mount primary culture were labeled with biotin. Biotinylated proteins were purified on streptavidin columns and identified by western blot. Figure 1B illustrates that a fraction of En1 and En2 is accessible to biotin, thus extracellular, and shows graded expression. Based on band intensities (Figure 1B, left panel), the percentage of extracellular Engrailed was evaluated to around 5% of total Engrailed. To further verify En1/2 extracellular localization, tissues were treated with proteinase K before biotinylation. Figure 1B (lower panel) demonstrates that this treatment does not affect intracellular proteins (RhoA) but fully degrades NCAM. It also shows that biotinylation only affects extracellular (proteinase K sensitive) proteins (biotinylated En1/2 and NCAM but not RhoA).

To verify the in vivo expression of extracellular En1/2, we used nonpermeabilized conditions for immunostaining on whole-mount *Xenopus* tecta with antibodies against En1/2 and the extracellular domain of NCAM. In these conditions, tecta showed positive immunostaining for Engrailed and NCAM. As illustrated and quantified in Figure 1C, En1/2 expression is graded, whereas NCAM staining is more evenly distributed. Indeed, the En1/2 fluorescent signal is 1.6 times higher in the posterior tectum than in the anterior with only a modest increase (1.1) in NCAM. En1/2 and NCAM exhibit a characteristic extracellular staining pattern nonoverlapping with the DAPI-stained nuclei (Figure 1C). Control experiments using an antibody against the intracellular protein, RhoA (Figure S1), demonstrate that permeabilized conditions produce strong RhoA cytoplasmic immunostaining that is uniformly expressed in the tectum (Figures S1A, S1C, and S1E). By contrast, nonpermeabilized conditions produce little RhoA immunostaining, although occasional, possibly damaged, cells are stained (Figures S1B, S1D, and S1F).

Taken together, these results demonstrate that a fraction of En1/2 is extracellular, tethered to the membranes, with a posterior-to-anterior expression that parallels that of nuclear En1/2.

In Vivo Extracellular Engrailed Contributes to A-P Topographic Mapping in *Xenopus*

To investigate whether extracellular Engrailed plays a role in retinal axon mapping in the tectum in vivo, we expressed single-chain antibodies to disrupt En1/2 nonautonomous activity in *Xenopus*. This approach was developed to block Pax6 nonautonomous activity in the zebrafish (Lesaffre et al., 2007) and consists of the expression of genetically encoded secreted single-chain antihomeoprotein antibodies. Engrailed 4G11 single-chain antibody, which recognizes En1 and En2, was cloned with or without a signal peptide (SP) for secretion (Lesaffre et al., 2007). The secreted and nonsecreted anti-En1/2 single-chain antibodies (SPsc4G11 and sc4G11, respectively) were tested for their specificity (Figure S2A), cellular localization (Figures S2B and S2D), association with Engrailed when expressed in vivo (Figure S2C), and ability to interfere with Engrailed transfer between cells (Figures S2E and S2F). When expressed by HEK cells, SPsc4G11 remains in the secretion pathway and does not reach the nucleus (Figure S2D), and 2 days later almost all of the antibody is extracellular (Figure S2B). Furthermore, SPsc4G11 in the culture medium decreases En2 intercellular transfer in vitro even in high En2 expression conditions (Figures S2E and S2F). In contrast, sc4G11 is not secreted (Figure S2B) and does not modify En secretion (data not shown).

Embryonic tecta were electroporated with single-chain antibody constructs at stages 28–32, after tectal polarity is established and 10–12 hr before the first retinal axons reach the tectum. Single-chain antibody expression was verified by myc-immunostaining (Figure S3A). At stages 43–45, the fluorescent lipophilic dyes, DiI (1,1′-dioctadecyl-3,3,3′,3′-tetramethylindocarbocyanine perchlorate) and DiO (3,3′-dioctadecyloxacarbocyanine perchlorate; Molecular Probes), were injected into the temporal and nasal parts of the retina, respectively, and the labeled axon terminals subsequently visualized in whole-mounted brains

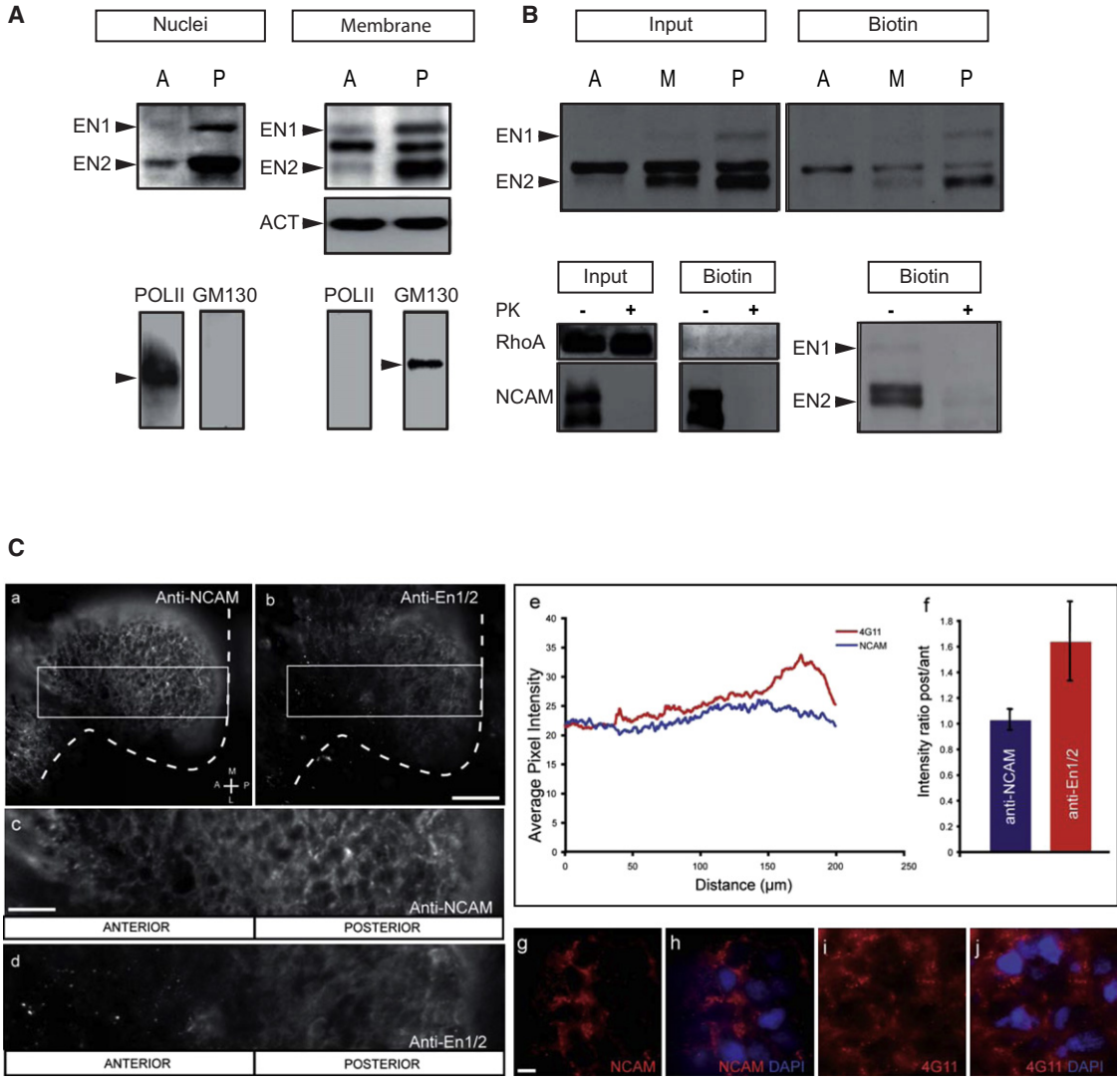

Figure 1. Engrailed Proteins Are Associated with Tectal Membranes in an A-P Gradient

(A) Chick Engrailed 1/2 proteins are associated with anterior (A) and posterior (P) membranes, which stain for ER/Golgi marker GM130 and actin. En1/2 is also present in nuclei identified by Pol-II. The equal intensities of actin and extracellular Hsc70 contaminant (migrating between En1 and En2) bands demonstrate that equal amounts of material were loaded in A and P slots.

(B) Tecta from E4 chick embryos were cultured (flat mount) for 1 day, and cell surface proteins were biotinylated. The proteins from anterior (A), median (M), and posterior (P) domains were extracted, and biotinylated proteins were retained on streptavidin columns. (Top panels) Total extracts (input) show a En1/2 graded expression also observed for surface (biotin) En1/2. (Bottom panels) Total input shows both extracellular (NCAM) and intracellular protein (RhoA). RhoA is not biotinylated, and only NCAM, not RhoA, is degraded by proteinase K (PK).

(C) Dorsal view of stage 37/38 flat-mounted *Xenopus* tecta showing extracellular immunostaining with antibodies to NCAM (Ca) and En1/2 (Cb). White dashed lines demarcate the posterior and lateral tectal border. Boxed regions in (Ca) and (Cb), shown at higher magnification below (Cc and Cd), indicate the rectangular area typically used for intensity plot quantification in (Ce) and (Cf). Retinal axon terminals (data not shown) are positioned in the anterior portion. (Ce) Pixel intensity per unit area was measured along the anterior-posterior axis (Engrailed-1/2, red; n = 5. NCAM, blue; n = 4), where zero value corresponds to the anterior tectal boundary. Bar graph (Cf) shows the ratios of mean intensity values of anterior versus posterior tectum (extreme 50 μm quadrants), which differs significantly between En1/2 and NCAM (Mann-Whitney U test). Data presented as means ± SEM. NCAM (Cg) and En1/2 (Ci) immunostaining (red) in the tectum appears extracellular/membranous in the nonpermeabilized conditions used and does not colocalize with nuclear DAPI (blue) signal (merged images in Ch and Cj). M, medial; L, lateral; A, anterior; P, posterior. Scale bars: (Ca and Cb) 60 μm, (Cc and Cd) 30 μm, (Cg–Cj) 8 μm.

Error bars indicate standard deviation.

(Figure 2). Each DiI/DiO injection yielded approximately three to eight labeled axons in the tectum. At these early stages of development, nasal and temporal axons overlap in the anterior-to-middle regions of the tectum, since both populations of axons enter the tectum anteriorly and course together to posterior destinations. A clear A-P separation between the two sets of axons is

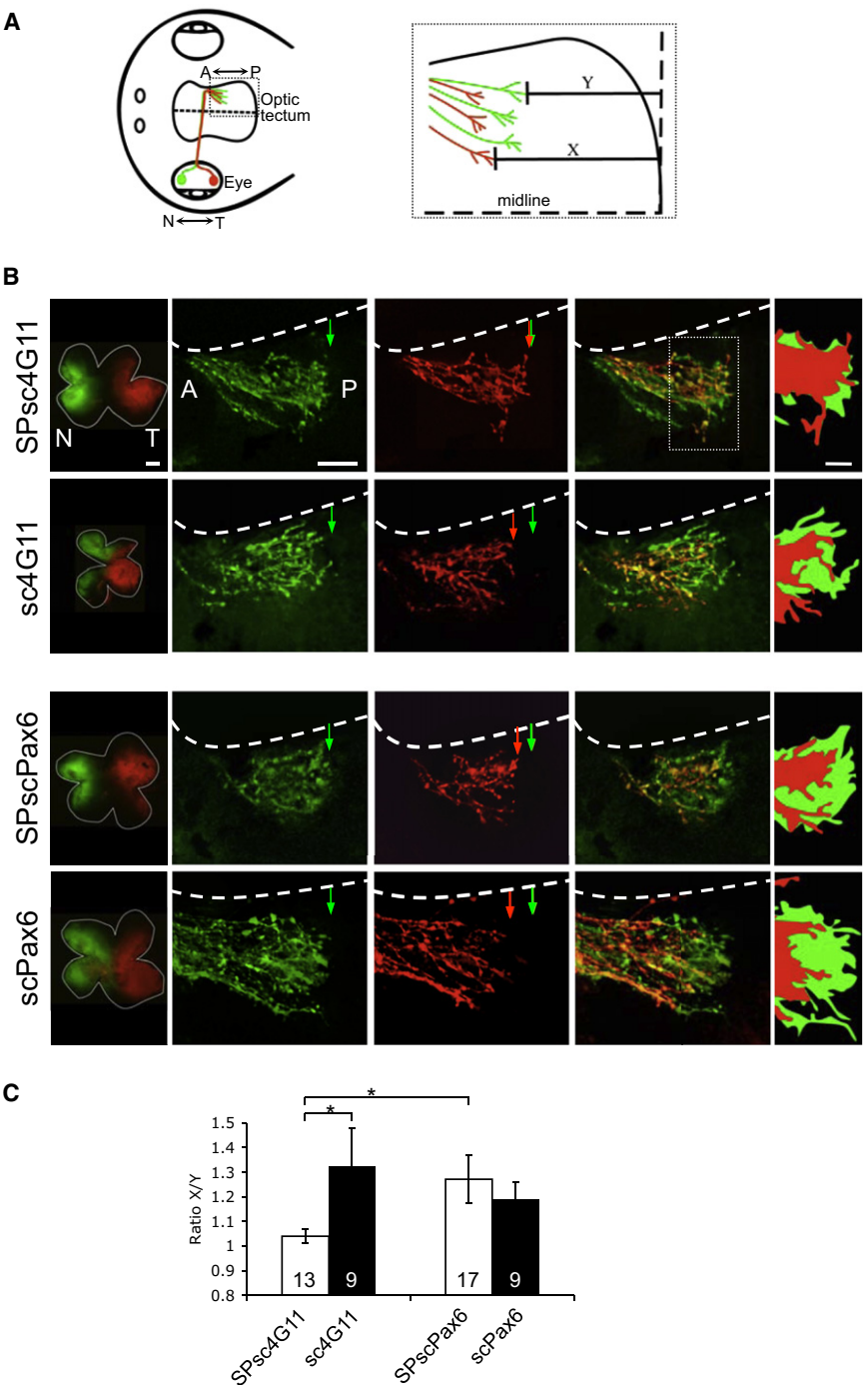

Figure 2. Tectal Expression of Single-Chain En1/2 Antibody Disrupts Mapping in *Xenopus*

(A) Schematic diagram of the *Xenopus* retinotectal projection (dorsal view). Nasal axons (green) project to the contralateral posterior optic tectum and temporal axons (red) to the anterior tectum. Area in dashed box is enlarged in the right panel. The topographic position of axon terminals was quantified by measuring the distance from the posterior tectal border (dashed vertical line) to the tips of temporal and nasal axons to give values X (temporal) and Y (nasal).

(B) Dorsal views of tecta showing anterogradely labeled retinal axons in single chain antibody-expressing tecta. Far left panel shows the sites of dye injection in flat-mounted retinas belonging to the tectal samples on the right. Temporal axons (red, DiI) extend aberrantly and as far as nasal axons (green, DiO) in tecta expressing SPsc4G11, but not in those expressing sc4G11, SPscPax6, and scPAX6. Position of the furthest extending nasal axon (green arrow) and temporal axon (red arrow) and lateral boundary of the tectum (white dashed line) are shown. Far right panels show a solid-filled outline of the two populations of axons to give a clearer visual representation of the degree of overlap. Scale bars: retina, 100 μm; tectum, 50 μm; outline tracing, 25 μm.

(C) Mean X/Y ratios in tecta expressing secreted (white) or nonsecreted antibodies (black). Normal topographic mapping gives a X/Y ratio > 1, whereas a lower ratio indicates topographic defects. Numbers in the bars denote the number of tecta analyzed. SPsc4G11 is significantly different from sc4G11 or SPscPax6 groups (*$p < 0.05$; Kruskal-Wallis test).

A, anterior; N, nasal; P, posterior; T, temporal. Error bars indicate standard deviation.

evident posteriorly where nasal axons extend 10–25 μm beyond temporal axons. The midbrain/hindbrain boundary, the isthmus, was taken as a stable landmark, and the distance between it and the posterior-most tips of temporal (X) and nasal (Y) retinal axons was measured (Figure 2A). This gave an X/Y ratio that could be compared across samples. In control samples, the X/Y ratio was greater than 1 (1.2–1.3), reflecting the lower axon-to-isthmus value of the more posterior-reaching nasal axons (Y).

Following SPsc4G11 expression, many temporal axons extended aberrantly into posterior territories, overlapping almost completely with nasal axons, and giving an X/Y ratio close to 1 (Figure 2). By contrast, when tecta were transfected with sc4G11, the X/Y ratio was 1.3, signifying normal A-P separation. Therefore, the effect of SPsc4G11 is likely through its secreted function. Expression of secreted or nonsecreted single-chain anti-Pax6 antibodies (Figures 2B and 2C) showed control X/Y values of 1.2–1.3, indicating that the SPsc4G11 result is not due to nonspecificity associated with the experimental approach.

Although SPsc4G11 does not escape the secretion pathway (Figure S2D) to reach the nucleus, it could be that undetectable amounts do so, neutralizing a sufficient percentage of nuclear En1/2 to downregulate EphrinA expression. This is unlikely, since single-chain antibodies are often inactive within cells, as the reductive intracellular milieu disrupts the disulfide bounds

necessary for antigen recognition (Auf der Maur et al., 2004; Strube and Chen, 2004). To verify the absence of cell-autonomous activity, SPsc4G11 and sc4G11 were electroporated into the *Xenopus* tectum, and EphrinA expression was visualized using EphA3-Fc (Cheng et al., 1995). Quantitative fluorescence analysis showed that although the average levels of EphrinA signal intensity showed a slight decline from wild-type, the values did not differ significantly from controls (Figures S3A and S3B), and the graded patterns of expression were not modified (Figures S3C and S3D). Since the amount of secreted antibody that escapes the secretion pathway, if any, is undetectable compared to that of the nonsecreted antibody (Figure S2), it is likely that the effects of SPsc4G11 on retinotectal mapping are non-cell-autonomous.

In Vivo Extracellular Engrailed Contributes to A-P Mapping in the Chick

The mechanism of topographic mapping in the visual system exhibits major differences between species (Dutting and Meyer, 1995; McLaughlin and O'Leary, 2005; Mueller et al., 1998). In *Xenopus* and fish, where the embryonic optic tectum is very small (250 μm A-P) at the time of initial innervation, axons grow directly to their correct destinations. In chick and mammals, with a tectum about ten times larger (2200 μm A-P), axons initially bypass their correct targets and later form interstitial branches in the correct location (O'Leary and McLaughlin, 2005). However, overshooting of axons is less pronounced in chick (Dutting and Meyer, 1995; Mueller et al., 1998).

In chick, tectal innervation takes place between E6 and E12. We thus electroporated chick midbrain at E4 with plasmids encoding SPsc4G11, sc4G11, or SPscPax6. Efficiency and site of expression were verified with GFP plasmid coelectroporation. Insertion of a DiI crystal into the most posterior visible part of the tectum at E11 retrogradely labeled retinal axons. The animals were fixed at E12, and the distributions of labeled retinal ganglion cells in retina whole mounts were compared. Experiments where the crystal was in the midregion of the tectum or where the GFP did not reach the posterior region of the DiI crystal were discarded.

In Figure 3A, the camera lucida drawings illustrate that SPsc4G11 induces more temporal RGCs to project into the posterior tectum than the other control conditions. This effect was quantified, showing an ~6-fold increase in the number of temporal axons projecting to the posterior tectum (Figure 3B). As in *Xenopus*, SPscPax6 and sc4G11 antibodies had no effect on temporal axons (Figure 3B). To verify the absence of non-cell-autonomous antibody activity, the expression of SPsc4G11, EphrinA2/5, and Pax7 was compared by RT-PCR in the SPsc4G11 electroporated and nonelectroporated sides of the tectum. As shown in Figure 3C, the expression of the antibody led to no significant modification in Ephrin-A2/5 or Pax7 expression. Finally, mRNA in situ hybridization experiments further illustrated the absence of effect of nonsecreted and secreted single-chain 4G11 on EphrinA2/5 or En1/2 expression at E3 (Figure 3D).

This series of experiments demonstrates that, also in the chick, axons from the temporal retina aberrantly invade the posterior tectum when extracellular Engrailed activity is disrupted.

Membrane-Associated Engrailed Is Required for Full Repulsion in Membrane Stripe Assay

When grown on alternating lanes of anterior/posterior tectal membranes, temporal axons extend preferentially on anterior membranes, exhibiting "striped outgrowth," due to the repellent activity of EphrinAs in the posterior membranes (Walter et al., 1987a). Since the neutralization of extracellular Engrailed causes mapping errors, we asked whether En1/2 also contributes repellent activity to posterior membranes. Striped carpets from anterior and posterior chick tectum membranes were produced (Walter et al., 1987a), and the presence of Engrailed protein was probed with two anti-engrailed antibodies (Figures 4A and 4B). Engrailed signal was high in the posterior membrane lanes and low in the anterior lanes, similar to that of EphrinA2 (Figures 4A–4C), confirming our biochemical data (Figure 1).

Next, nasal and temporal strips of E6 chick retinas were placed perpendicular to the membrane stripes, and the outgrowth of the retinal ganglion cell (RGC) axons was scored 2 days later. As expected (Walter et al., 1987a; Yates et al., 2001), temporal fibers grew preferentially on membranes from anterior tectum (Figure 4D), whereas nasal fibers grew randomly on anterior and posterior membranes (data not shown). To investigate a putative En1/2 role, we used specific blocking antibodies. Posterior membranes were incubated with one polyclonal (86.9 [Sonnier et al., 2007]) and two monoclonal (4D9 and 4G11) antibodies against En1/2 proteins or with a control antibody to Otx2 prior to preparing the membrane carpets. Growth preferences were evaluated blindly by two independent observers (A.W. and L.S.) using a scoring system ranging from 3 for a very strong preference to 0 for no preference for anterior membranes.

Blocking En1/2 activity with any of the three anti-Engrailed antibodies reduced temporal repulsion (Figures 4E and 4H). Axons still showed a preference for anterior membranes, but the striped pattern was "blurred" due to axons straying into posterior membrane lanes (Figure 4E). Indeed, the overall preference of temporal axons for anterior membranes was reduced to an average score between 1 and 1.7 compared to 3 for wild-type (Figure 4H). The activity of the 4D9 antibody was neutralized by preincubation with the Engrailed homeodomain, which contains the epitope recognized by this antibody but has no activity per se (Brunet et al., 2005). Antibodies against Otx2 (Figures 4G and 4H) or Pax6 (data not shown) did not change the preference of temporal axons for anterior membranes, although Otx2 is also present in the membrane fractions (data not shown).

To further test whether extracellular Engrailed influences temporal axon choice, we used membranes derived from the SC of newborn *En1*$^{-/-}$ mutant mice (Wurst et al., 1994). En1 is absent and En2 protein is severely reduced in these mice (Figure S4A). We found that *En1*$^{-/-}$ posterior tectal membranes lost most of their ability to repel temporal axons (Figures S4A and S4B) despite the continued (although reduced) expression of EphrinA2/A5 at the mRNA and protein levels (Figure S4C). Quantification of repulsion (blind observation, two independent observers) is shown in Figure S4B. An explanation is that Ephrin concentrations in the mutant are reduced to levels not allowing temporal growth cone repulsion. However, in the light of our results supporting a direct nonautonomous activity of En1/2, it

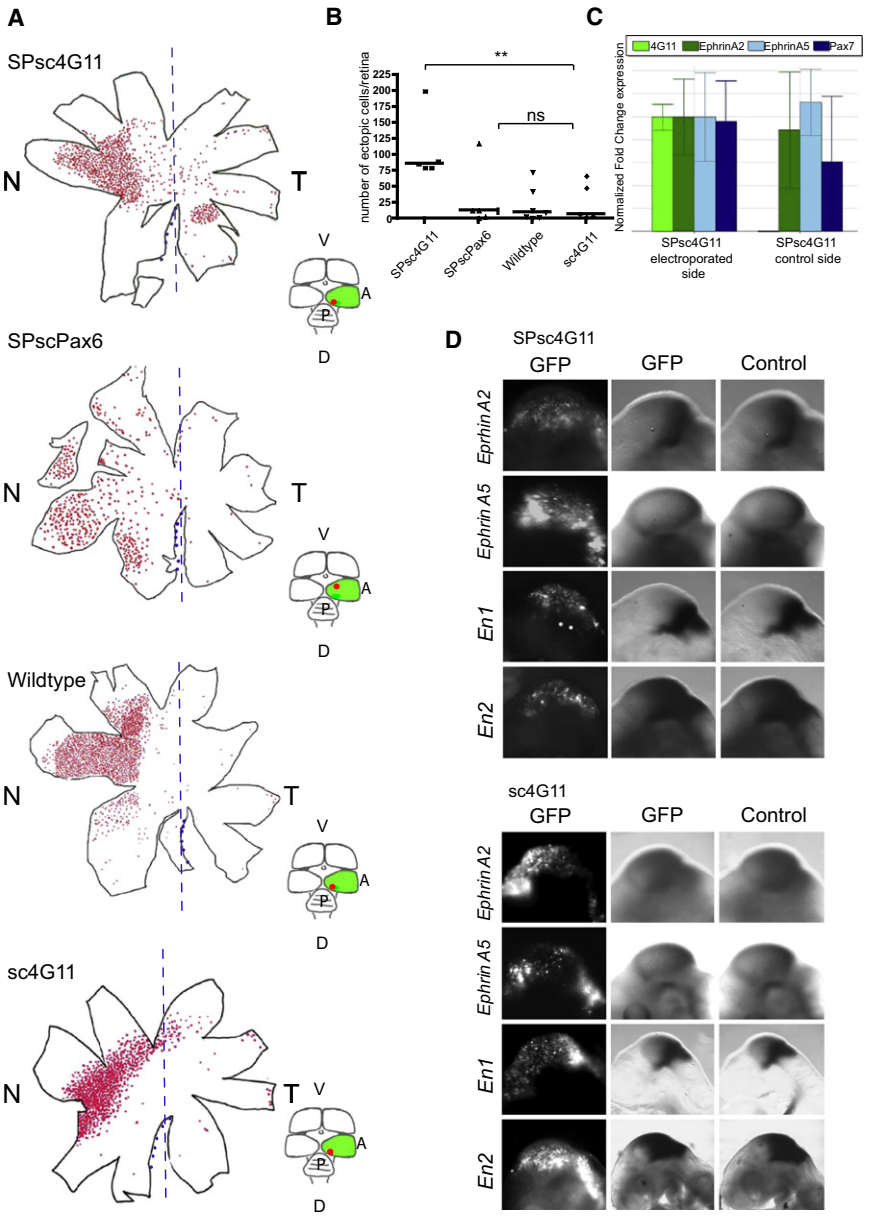

Figure 3. Interfering In Vivo with Engrailed Intercellular Signaling Disrupts Topographic Mapping in Chick

(A) Temporal retinal ganglion cells were labeled by insertion of a DiI crystal in the posterior tectum expressing SPsc4G11, sc4G11, SPscPax6, or none of those (WT). To the left are camera lucida drawings of retinas where retrogradely labeled ganglion cells are indicated by red dots. The retinas are oriented with dorsal at the top, nasal (N) at the left, and temporal (T) at the right. The scheme of the brains to the right of the retinas shows the placement of the DiI crystal in the posterior part of the tectum (at that time the chick tectum has turned 90°, thus the posterior end becomes located toward the middle of the brain).

(B) Quantification of misplaced temporal projections show that in tecta transfected with SPsc4G11 a significantly higher portion of temporal retinal cells was labeled (Student's t test).

(C) E4 tecta were electroporated at E4 with the SPsc4G11-expressing plasmid, and the effect of this expression on EphrinA2/5 and Pax7 expression was analyzed at E5 by RT-PCR. This figure illustrates the unilateral expression of the antibody (4G11) and the equal amounts of EphrinA2/A5 and Pax7 in the electroporated and contralateral sides.

(D) Chick tecta were electroporated at E2 with plasmids encoding SPsc4G11 or sc4G11 and fixed at E3. Whole-mount RNA ISH against EphrinA2, EphrinA2, En1, and En2 were performed. The expression patterns of Ephrin and Engrailed mRNA on the side transfected with SPsc4G11 (upper picture) and sc4G11 (lower picture) are shown in the GFP expressing tectum (first and second row of pictures). The last row of pictures shows the mRNA expression of the non-electroporated side.

Error bars indicate standard deviation.

is also possible that the sensitivity of temporal growth cones to Ephrins is reduced at low Engrailed concentrations. This led us to investigate whether Engrailed could increase the sensitivity of temporal axons to low EphrinA5 levels.

Engrailed Increases Axon Sensitivity to EphrinA5

The experiments reported above do not discriminate between En1 and En2, and only En2 was shown previously to repel temporal axons (Brunet et al., 2005). We thus needed to verify the ability of En1 to repel temporal growth cones. Figure S5 illustrates that En1 and En2 have the same ability to repel *Xenopus* temporal growth cones in the turning assay. This experiment reinforces the idea that Engrailed may have a role in mapping. Because of the experiments obtained with the stripes from En1-invalidated mice and the large body of literature establishing a function for Ephrins in guidance (Flanagan, 2006), we wondered whether Engrailed and the EphrinA system may have evolved a cooperative function.

We first determined the minimal concentration of EphrinA5 required to elicit striped temporal axon outgrowth. We found that lanes of EphrinA5 at a concentration of 0.1 μg/ml did not cause detectable striped outgrowth, whereas 8 μg/ml concentration (standard concentration in this assay [Ciossek et al., 1998]) caused robust striped outgrowth, with 85% of the axons avoiding the EphrinA5 lanes (Figures 5A and 5B). At 0.5 μg/ml, about 30% of the temporal axons exhibited clear striped outgrowth, and the rest grew randomly across the lanes (Figures 5A and 5B). Thus 0.1 μg/ml was identified as the "subthreshold" concentration and 0.5 μg/ml EphrinA5 as the "minimal" concentration for striped outgrowth. When soluble En2 at a 75 nM concentration was added globally to the medium with the subthreshold 0.1 μg EphrinA5 lanes, striped outgrowth occurred

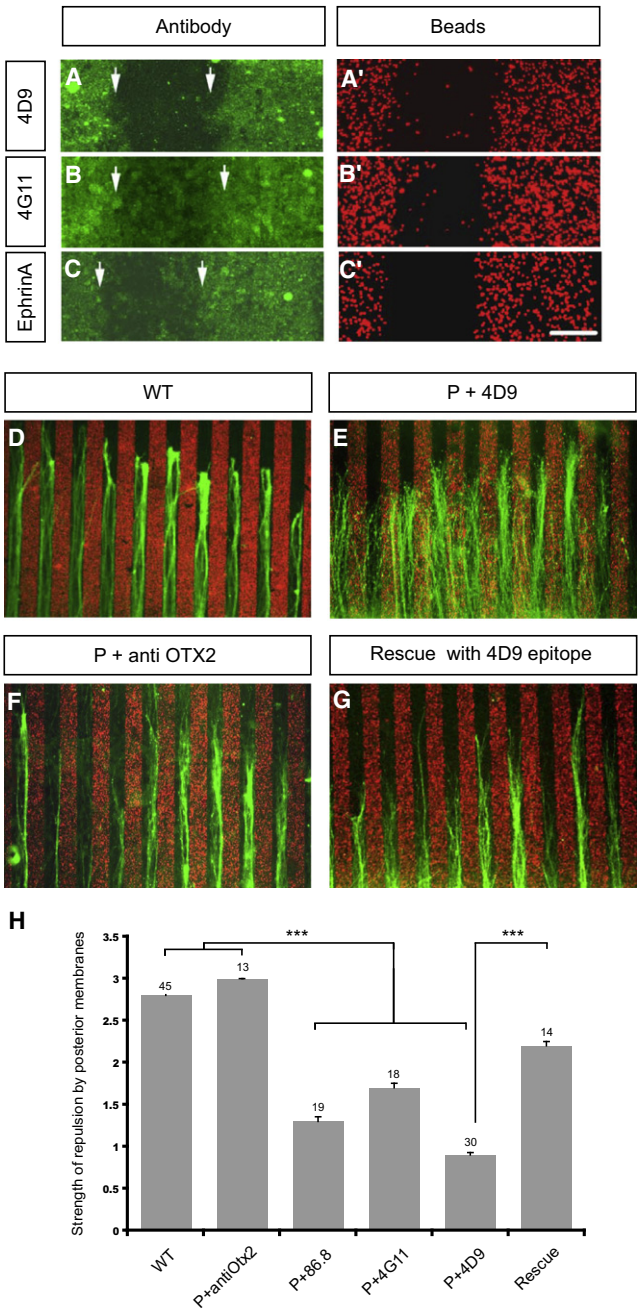

Figure 4. Engrailed Is Necessary for Full Temporal Cone Repulsion in the Stripe Assay

(A–C') Alternating lanes of anterior and posterior membranes were stained with 4D9 (A) and 4G11 (B) anti-Engrailed antibodies and with an anti-EphrinA2 (C) antibody. The fluorescent beads (carboxylate-modified microspheres 0.5 μm, red fluorescent from Molecular Probes) (A'–C') indicate posterior membranes. Arrows in (A)–(C) show the border between posterior and anterior membrane stripes. Scale bar, 45 μm.

(D–G) Axonal outgrowth of temporal axons in stripe assays, where posterior membranes were untreated (D), preincubated with the 4D9 anti-Engrailed antibody (E), the anti-Otx2 antibody (F), or the 4D9 antibody neutralized with the epitope (G). Preincubation of posterior membranes with the Engrailed antibody blurred the anterior preference of temporal axons (E), the Otx2 antibody had no effect (F), and neutralizing the Engrailed antibody restored a normal growth pattern (G). Posterior is in red; anterior is in black.

(H) Quantification of temporal (T) repulsion (3 for maximal repulsion, 0 for no repulsion). Anti-Otx2 had no effect compared to WT. The polyclonal (86.8) and the two monoclonal anti-En1/2 antibodies (4G11 and 4D9) reduced the repulsive effect of posterior membranes on temporal axons to a score of 1.5 (Mann-Whitney test, ***$p < 0.001$ for each control column compared to each anti-Engrailed treated column). Neutralizing the 4D9 antibody with its epitope restored repulsion (rescue, ***$p < 0.001$, Mann-Whitney test). Numbers in parentheses indicate the number of explants analyzed. Analysis of variance showed a significant group effect ($p < 0.001$, ANOVA test).

Error bars indicate SEM.

at levels slightly higher than that elicited by the minimal 0.5 μg/ml concentration (50% versus 35%) (Figures 5A and 5B). This indicates that En2 increases the sensitivity of temporal axons to EphrinA5.

The stripe assay takes 48 hr; thus, the effects of En2 on axon growth may be indirect. To better analyze the cooperation between En2 and EphrinA5, we used the growth cone collapse assay that responds within 10 min. The standard EphrinA5 concentration (10 μg/ml) induced collapse in 80% of the temporal growth cones, whereas a subthreshold dose of EphrinA5 (0.1 μg/ml) did not raise collapse above the 20% control value (Figure 5C). En2 protein alone at a concentration of 75 nM did not induce collapse above control levels, but raised it to 75% of the growth cones in the presence of the subthreshold EphrinA5 level (0.1 μg/ml) (Figure 5C). Preincubation of En2 with a neutralizing antibody (4D9) or the use of a noninternalized mutant (EnSR [Brunet et al., 2005]) did not increase collapse above "sub-EphrinA5" values. Finally, α-amanitin (transcription inhibitor) did not inhibit the En2/EphrinA5 cooperative interaction, but anisomycin (translation inhibitor) did. Full EphrinA5 activity was only partially affected by anisomycin. These results suggest that the cooperative effect between En2 and EphrinA5 depends on En2 regulating the translation of one or several factors that allow the growth cones to respond to subthreshold EphrinA5 concentrations. Together with the stripe assay data, the growth cone collapse results suggest that extracellular En2 increases the sensitivity of retinal axons to EphrinA5.

DISCUSSION

This study provides several lines of evidence supporting the idea that extracellular Engrailed plays a role in retinotectal patterning. First, 5% of total En1/2 proteins are associated with the extracellular side of tectal membranes with graded A-P expression. Second, posterior membranes deprived of part of their active Engrailed content show reduced repulsion for temporal axons. Third, En2 increases the sensitivity of retinal axons to EphrinA5. Finally, the in vivo neutralization of extracellular En1/2 in the tectum leads to aberrant posterior projections of temporal axons in two different species.

The finding that posterior membranes from mutant *En1*$^{-/-}$ tecta fail to cause striped outgrowth from temporal retina suggests that membrane-attached En1 participates in posterior membrane repellent activity. This is at odds with the findings that lanes of EphrinA induce robust striped outgrowth in the absence of Engrailed and that, while EphrinA2/A5 are expressed in mutant

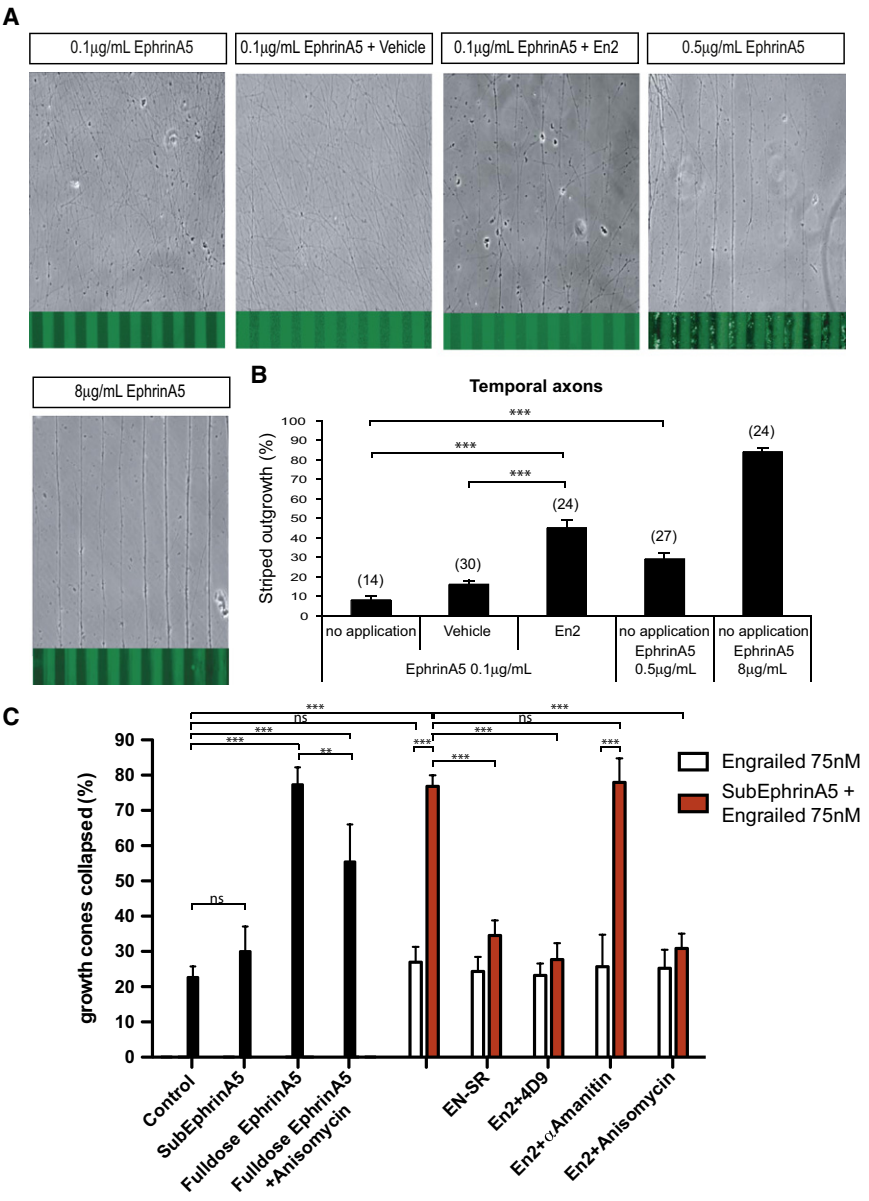

Figure 5. EphrinA5 and En2 Cooperate In Vitro for Axonal Guidance and Growth Cone Collapse

(A) Top panels illustrate typical random outgrowth observed with subthreshold (0.1 µg/ml) EphrinA5 concentration and demonstrate that the addition of En2 at a 75 nM concentration but not of the vehicle (En2 buffer) restores striped outgrowth, comparable with the striped outgrowth pattern observed at 0.5 µg/ml EphrinA5. The bottom picture shows clear striped outgrowth obtained with high EphrinA5 (8 µg/ml). EphrinA5 is in green.

(B) Quantification of striped outgrowth observed when axons are growing on three different EphrinA5 concentrations (0.1 µg/ml, 0.5 µg/ml, and 8 µg/ml). At 0.1 µg/ml, growth is almost entirely random, whereas at a 0.5 µg/ml concentration, 1/3 of the axons show a striped outgrowth pattern. Adding En2 in the medium of axons growing on 0.1 µg/ml EphrinA5 increases the percentage of axons that show striped outgrowth to a value similar to that observed on 0.5 µg/ml EphrinA5. Numbers in parentheses indicate the number of experiments. ***$p \leq 0.0001$ using Student's t test.

(C) Chick temporal axons were submitted to a collapse-inducing (full-dose EphrinA5) concentration of EphrinA5 (10 µg/ml) or to a concentration of 0.1 µg/ml that has no effect per se (sub-EphrinA5). Growth cone collapse was tested in the presence of En2 alone (empty bars, 75 nM) or of EphrinA5 (0.1 µg/ml) plus En2 (75 nM) (red bars). This graph illustrates how En2 lowers the threshold of EphrinA5-induced collapse. Noninternalized En2 (EnSR) or antibody-neutralized En2 are without effect. En2 activity is translation dependent and transcription independent. Full-EphrinA5 activity is partially translation dependent. Experiments were repeated three to six independent times, and the total number of growth cones counted for each condition range between 600 and 2400 (***$p \leq 0.0022$ and **$p \leq 0.0043$, Mann-Whitney two-tailed U test).

Error bars indicate standard deviation.

En$^{-/-}$ tecta, their levels are reduced. Therefore, it could be that *En1*$^{-/-}$ membranes do not have sufficient amounts of Ephrins to cause repulsion. Alternatively, normal Engrailed expression might be needed for EphrinA-induced striped outgrowth.

Ectopic overexpression of En1 (Logan et al., 1996) or En2 (Friedman and O'Leary, 1996) in the embryonic chick optic tectum repels temporal axon growth. This repulsion was interpreted as being due to the induction of EphrinAs by En1/2. Our current and previous results (Brunet et al., 2005) suggest an additional mechanism whereby Engrailed directly influences the behavior of temporal retinal axons. Although the present study does not allow us to analyze separately the roles of En1 and En2, we verified that the two molecules can repel temporal axons and attract nasal ones (En1 attraction data in legend to Figure S5) and thus have similar guiding activities.

The presence of Engrailed in the isolated tectal membrane fractions confirms previous observations (Joliot et al., 1997). In addition, we show here that the two proteins are accessible to extracellular reagents, such as biotin or proteinase K. Interestingly, extracellular Engrailed is tethered to the membranes, a finding that may explain why the graded nuclear expression is preserved in membrane preparations. This behavior is reminiscent of that observed for many morphogens that are tethered extracellularly by complex sugars (Bovolenta, 2005).

To be active in vitro, En2 must be captured by the growth cones and imported into the cytosol where it regulates protein synthesis through the mTOR pathway (eIF4E-dependent capped mRNA translation initiation) (Brunet et al., 2005; Gingras et al., 1999). We do not know whether this is also the case in vivo, as Engrailed may also act directly on receptors expressed by the

growth cones. It will thus be important in the future to identify the Engrailed signaling pathways and the mRNAs that are translated upon Engrailed presentation. Otx2, which is also present in the membrane fraction, showed no repulsive activity in the turning assay for RGC growth cones (Brunet et al., 2005), and Otx2 antibodies had no effect in the stripe assay. These results further confirm the specificity of the Engrailed signaling mechanism.

The exuberance of guidance molecules already identified could mask redundancy, true physiological and mandatory interactions, or interactions not absolutely necessary but bringing robustness to the system (Brunet et al., 2007; Holcman et al., 2007). Redundancy is well illustrated by a recent study on triple EphrinA (A2/A3/A5) and double EphrinA (A2/A5) plus β2 subunit of the nicotinic acetylcholine receptor (A2/5/β) mutants (Pfeiffenberger et al., 2006). These studies demonstrated that retinotectal topography is severely disrupted in the EphrinA2/A3/A5 knockout and "nearly absent" in the EphrinA2/A5/β mutant. However, patterning is not completely absent in either mutant. There is thus, in addition to EphrinAs, space for other factors, including factors secreted by tectal cells through an activity-dependent mechanism requiring intact nicotinic receptors.

Molecular cooperation in vivo contrasts with many in vitro experiments in which guidance or collapse is elicited by individual factors. It could be that such in vitro assays only work when the concentration of candidate proteins is above physiological values. This is possible for Engrailed in the turning assay (Brunet et al., 2005), but also for EphrinA5 (this report). Indeed, full repulsive activity is observed at 8 μg/ml but not at 0.1 or 0.5 μg/ml. In addition, at 0.5 μg/ml some axons grow on and others off the stripes (data not shown), suggesting axonal heterogeneity (Hansen et al., 2004; Weinl et al., 2005).

En2 added to 0.1 μg/ml ephrin-A5 stripe cultures induces a 0.5 μg/ml-like pattern of axon growth and suggests the existence of cooperative interactions between En2 and Ephrin-A5, confirmed in the collapse assay. This interaction is unlikely to be physical (Figure S6) and requires translation but not transcription. Although growth cone collapse and growth on membrane stripes are distinct behaviors with different time constants (10 min and 48 hr, respectively), the hypothesis that Engrailed acts at the level of local translation on membrane stripes is in agreement with our previous finding that Engrailed activity requires its internalization by growth cones and local protein translation (Brunet et al., 2005). One possibility is that En2 elicits the local translation of EphA receptors that leads to increased EphrinA sensitivity through increasing the numbers of surface receptors. However, our preliminary experiments have failed to detect an Engrailed-induced increase in EphA3 receptor expression in *Xenopus* retinal growth cones (data not shown). To better understand the nature of the Engrailed-EphrinA "interaction," we have started a systematic study to identify En1/2 translation targets. Among the candidates identified so far, more than 50% are associated with mitochondrial activity and ATP synthesis (our unpublished data).

An important observation in the present study is the defect in temporal axon guidance when extracellular Engrailed is neutralized in the posterior tectum in vivo. Our data do not show an attraction of nasal axons by Engrailed, although this cannot be totally excluded. Expressing single-chain antibodies in the extracellular milieu has the enormous advantage not to modify the levels of Engrailed expression within producing cells. Analysis of EphrinAs expression in *Xenopus* and of EphrinAs, En1/2, and Pax7 in the chick yielded no detectable changes, indicating that secreted En1/2 did not exert its effect on axon targeting through altering the transcription of key topography genes. However, since the expression analysis was performed 1 day after electroporation in the chick, the possibility that changes in gene expression occurred subsequently cannot be excluded.

The finding that extracellular En1/2 plays a direct role in retinotectal patterning in vivo does not preclude a critical role for other guidance molecules. We speculate that the complexity of interactions at work makes it likely that, if none of the candidates is sufficient to ensure axonal guidance (in physiological concentrations), some might be necessary. This is the case for EphrinAs, since the A2/A5 and the A2/A3/A5 mutants are severely disrupted (Pfeiffenberger et al., 2006). This might also be the case for En1/2, as neutralizing anti-Engrailed antibodies disrupt the pattern of axonal elongation in vivo.

In conclusion, the in vivo single-chain antibody approach has allowed us to demonstrate an Engrailed axon mapping function associated with its secretion and probably involving local translation. The extracellular involvement of Engrailed protein in guiding axon growth in vivo is reminiscent of the extracellular role shown for other homeoproteins such as Pax6 and Otx2 in eye development (Lesaffre et al., 2007) and critical period regulation (Sugiyama et al., 2008) and suggests that non-cell-autonomous activity of homeoproteins may be involved in multiple aspects of CNS development.

EXPERIMENTAL PROCEDURES

Antero-Posterior Fractionation of Tectal Cells

Membranes from E9 chick tectum were prepared as in Walter et al. (1987b). Nuclear pellets were treated with 0.5% NP40 in PBS with protease inhibitors (IP), 15 min, 4°C, rinsed twice with PBS IP, and suspended in PBS IP. Membrane fractions loaded on a sucrose step gradient (1.7 M/0.25 M) were centrifuged (30 min, 100,000 × g, 4°C). Interface material was centrifuged (30 min, 100,000 × g, 4°C) and suspended in PBS IP. Equal amounts of total proteins (BIORAD) of anterior and posterior membrane and nuclear fractions were analyzed by western blotting.

Cell Surface Biotinylation, Proteinase K Treatments

Biotinylation on open book cultures was conducted according to PIERCE kit (ref: 89881). Separate domains of E9 chick tecta were cultured for 1 day on tissue culture inserts 0.4 μm pore size (MILLIPOREPICMORG 50). For PK treatments, posterior tecta from E9 chick embryo were cultured for 1 day at 37°C and treated with PK (FERMENTAS) at 1 mg/ml for 10 min at 4°C. PK activity was stopped with PMSF. Proteins were extracted, loaded on streptavidin beads, and eluted.

Western Blots

Antibodies: anti-Engrailed antibody 86.8 (1/5000) (Sonnier et al., 2007), anti-Otx2 rat monoclonal antibody (1/5000) (Sugiyama et al., 2008), anti-RNA Polymerase II (monoclonal 1/1000, CTD4H8, UPSTATE, 05-623), anti-GM130 (monoclonal 1/250, Transduction Laboratories, G65120), anti-β-actin (monoclonal antibody 1/5000, SIGMA, A1978), anti-RHOA (monoclonal 1/500, SANTA-CRUZ, sc-418), polyclonal anti-NCAM antibody (1/4000), provided by Dr. C. Goridis. Secondary antibodies were HRP conjugated anti-rabbit (1/5000), anti-mouse (1/5000), or anti-rat (1/5000) (Amersham Lifescience). Peroxidase activity was revealed using ECL (Amersham).

En1$^{-/-}$ Knockout Mice

See legend to Figure S4.

Xenopus Retinal Explant Culture and Growth Cone Turning Assay

See legend to Figure S5.

Membrane Stripe Assay

Membranes, striped carpets, and retina were prepared as in Knoll et al. (2007) and Walter et al. (1987a). In short, SCs/Tecs (E18 to newborn/embryonic day 9, respectively) were divided into anterior and posterior parts. Membranes (OD 0.1 at 220 nm) were sequentially sucked onto a nucleopore filter in 90 μm stripes. Prelabeled (10 μl DiASP stock in 2 ml HBBS; DiASP stock: 5 mg/ml) retina strips (300 μm) were placed perpendicular onto the membrane stripes with metal weights. Retinas were cultured for 2 days (F12, with 10% FCS, GIBCO), fixed in 4% PFA, and mounted (glycerol/PBS 10:1) before evaluation.

Collapse Assay

The collapse assay was performed as described (Raper and Kapfhammer, 1990). Retinal explants (E7) were grown overnight on laminin (20 μg/ml) coated coverslips. En2 and EnSR (75 nM) were added as described in the text. When indicated, 10 μM anisomycin (Sigma) or 10 μg/ml α-amanitin (Calbiochem) were applied immediately prior En2 and EphrinA5. Cultures were fixed (4% PFA) after 10 min. The growth cones were observed blind (inverted phase-contrast microscope). Collapse was defined as no lamellipodia and two filopodia or less.

Antibody Treatment of Membranes

Pax6, 4D9, 4G11 antibodies (Developmental Hybridoma Bank, Iowa City, IA, USA), and anti EphrinA2 (Abcam) were added to chick posterior membranes at a concentration of 0.2 μg/ml and shaken for 1 hr at 4°C. Rat anti-Otx2 (Sugiyama et al., 2008) and rabbit anti-Engrailed (Di Nardo et al., 2007; Sonnier et al., 2007) were used at a 1/1000 dilution.

EphrinA5 Striped Substrates

Striped carpets of purified ephrinA5 were produced as described (Hornberger et al., 1999; Knoll et al., 2007; Vielmetter et al., 1990). After 8 hr of culture, Engrailed was added at a concentration of 1 μg/ml for 16 hr before fixation (PFA 4%) and analysis. Striped outgrowth was quantified by counting the lanes occupied by axons in general, divided by the lanes containing axons with striped outgrowth (number in brackets show number of axons analyzed).

mRNA In Situ Hybridization and EphA3-Fc Stainings

ISH was carried out as in Wilkinson and Nieto (1993) using [^{35}S]CTP-labeled single-stranded RNA probes or digoxygenin-UTP-labeled single-stranded RNA probes. EphA3-Fc staining was conducted as in Cheng et al. (1995).

Single-Chain Antibody Plasmids

Single-chain antibody plasmids were prepared from total RNA of anti-Engrailed 4G11 and anti-Pax6 hybridomas (Developmental Hybridoma Bank, Iowa City, IA, USA). The sequences were cloned downstream of an EF1α promoter, with or without signal peptide (Lesaffre et al., 2007). Poly-histidine and myc tags were added in C terminus.

Electroporation of *Xenopus* Optic Tectum

The dorsal midbrain of stage 28–31 *Xenopus* embryos was electroporated as described (Falk et al., 2007). Plasmids (1.8 μg/μl) were injected into the third ventricle and electroporated (eight pulses, 50 ms/18 V, 1 s interpulse). Embryos were raised at 18°C until stage 43–45, fixed in PFA 4% at room temperature either for 1–2 hr for anterograde labeling or for 30 min for EphrinA staining.

Anterograde Lipophilic Dye Labeling of Nasal and Temporal Retinal *Xenopus* Axons

Nasal and temporal parts of the retina of PFA-fixed stage 43–45 embryos were injected with DiO (in DMF [N,N-dimethylformamide] 25 mg/ml, Molecular Probes) and DiI (in 100% ethanol) in micropipettes (DiO: 1.0 mm OD × 0.78 mm ID, GC100TF10, Harvard Apparatus; DiI: 1.0 mm OD × 0.5 mm ID, 27-30-1, Frederick Haer & Co; puller: Pul-1, World Precision Instrument) using a Picospritzer (General Valve). Dye-injected embryos were kept at 25°C in PBS for 3 days to allow dye diffusion.

Immunohistochemistry and EphrinA Staining

Myc Antibody and EphA3-Fc Staining

Xenopus embryos were fixed (4% PFA, 1 hr at RT). Following DiI/DiO retinal labeling, the brains were dissected and processed as whole mounts. DiI/DiO-labeled tecta were first mounted in PBS for image capture and then processed for antibody staining with permeabilization. Brains were blocked for 1 hr with 5% goat serum and incubated overnight in primary antibodies at 4°C. Primary antibodies used were monoclonal mouse anti-myc (clone 9E10, 1:2000, Sigma) or polyclonal rabbit anti-myc (1:2000, AbCam) diluted in PBS plus 5% goat serum. After PBS washes, tissue was incubated overnight in secondary antibody at 4°C. Secondary antibodies diluted in PBS plus 5% goat serum were goat anti-mouse Cy3 (1:2000, Chemicon), goat anti-human Cy3 (1:2000, Jackson ImmunoResearch), or goat anti-rabbit Alexa Fluor 488 (1:1500, Molecular Probe). Tecta were mounted in PBS with or without glycerol (CitiFluor). For myc staining, PBS blocking solution and antibody diluents were supplemented with 0.1% Triton X-100 (Sigma). The EphrinA distribution in the optic tectum was visualized on nonpermeabilized whole-mount *Xenopus* brains using recombinant mouse EphA3/human Fc chimera (8 μg/ml, R&D Systems) and recombinant human IgG Fc as negative control.

Extracellular Engrailed Immunostaining

Stage 37/38 *Xenopus* embryos were anesthetized in MS222 (3-aminobenzoic acid ethyl ester methanesulphonate salt, Sigma), the optic tecta were surgically exposed as described (Chien et al., 1993; Strochlic et al., 2008) and lightly fixed for 10 min in 4% PFA. Immunostaining was performed under nonpermeabilized conditions (Furrer et al., 2007), with minor modifications. Embryos were washed and incubated overnight in primary antibodies at 4°C. Antibodies used were anti-Engrailed (4G11, DSHB), anti-neural cell adhesion molecule (NCAM, 6F11; Sakaguchi et al., 1989) at 1:20 and anti-RhoA (SC-179, Santa Cruz Biotechnology) at 1:1000, in PBS plus 5% goat serum. Embryos were blocked for 1 hr with 5% goat serum and incubated for 2 hr with goat anti-mouse Cy3 (1:1000) and postfixed for 30 min in 4% PFA. Brains were counterstained with the nuclear marker 4′-6-diamidino-2-phenylindole (DAPI, diluted 1:10,000, Sigma) and mounted in FluorSave (Calbiochem).

Electroporation of Chick Tecta and DiI Staining

E2 chick tecta were electroporated as described (Haas et al., 2001). E4 embryos were cultured in Petri dishes (Auerbach et al., 1974) for easier access. Plasmids (2 μm/μl) containing the single-chain antibodies and GFP containing pCAX (1.5 μg/μl) (Swartz et al., 2001) were injected into the fourth ventricle, and electrodes were placed left and right of the midbrain at E2 and electroporated (five pulses, 50 ms, 17–20 V). At E4, prewarmed Tyrode's + penicillin/streptomycin (GIBCO) was used to raise the fluid around the head. Then the head was further raised with forceps to allow positioning the electrodes below and above the midbrain. Embryos were incubated until the required stages and transfection was verified under a fluorescence microscope.

Quantitative RT-PCR

Total cellular RNA was extracted from the electroporated area or the equivalent contralateral side using RNeasy MicroKit (Quiagen). Hundreds of nanograms of purified total RNA were used to generate first-strand cDNAs using random primers and Superscript III enzyme (Invitrogen). QPCR was performed (iCycler Real-Time PCR detection system [Bio-Rad]) using iQ SYBR Green PCR Supermix (Bio-Rad). PCRs were performed in duplicate using 1 μl of cDNA (total volume of 25 μl). Each sample was normalized with β-actin, GAPDH, and HPRT. Primers were as follows: chick EphrinA5, 5′-ACCGCTA CGCCGTCTACTGGA-3′ and 5′-CACGGGATGGCTCGGCTGACTC-3′; chick EphrinA2 5 -CCACCGCGGGGATTACACC-3′ and 5′-AAGAGCCCAGCAGAGT CCAGAAGA-3′; chick Pax7 5′-GCGCCCACTGCCCAACCACATC-3′ and 5′-C TGCGGCGCTGCTTCCTCTTCAAA-3′; 4G11 primers (4G11QprimL3, 5′-GCC AGTCTCCTAAACTGCTGAT-3′ and 4G11QqprimR3, 5′-TGCTGATGGTGAAA GTGAAATC-3′); chick GAPDH (BL34, 5′-ACCAGGTTGTCTCCTGTGACTT-3′ and BL35, 5′-ACACGGTTGCTGTATCCAAACT-3′), chick HPRT (BL36 5′-ACGCCCTCGACTACAATGAATA-3′ and BL37 5′-GCTTTGTAGCCATAGC

ACTTCA-3′); chick β-actin from Quiagen QuantiTect Primer Assay numer QT00600614.

Retrograde Labeling of Chick RGCs

RGCs were labeled with DiI crystals (Molecular Probes) placed close to the exposed caudal tectal pole of embryos at E11 (Thanos, 1991). After 30 hr, the brain and the eyes were removed and fixed in 4% PFA. Retinas were flat mounted on glass slides, covered with glycerol:PBS (9:1). DiI-stained RGCs in the temporal retina were counted (20× objective). After photographing the location of the DiI crystal in the tectum, midbrains were embedded in 3% agarose, cut into 80–100 μm sections with a vibratome, embedded in glycerol, evaluated, and photographed with a Zeiss LSM 500.

Imaging and Quantification in *Xenopus*

Xenopus brain samples were visualized (Nikon Optiphot inverted microscope) using 10× (Nikon Plan Apo, 0.45), 20× (Nikon Plan Apo, 0.75), and 100× (Nikon Plan Apo, 1.40 oil) objectives. Images were captured with an Orca-ER Hamamatsu CCD camera using Openlab 4.0.2 software (Improvision, Lexington, MA). For high-resolution images, tecta were imaged at 20× magnification (Leica MPC confocal microscope). Measurements were performed using Openlab. Transfection efficiency was assessed using immunofluorescent detection of myc on whole-mount brains (McFarlane et al., 1996). Only tecta with widespread myc-positive cells were included for analysis.

Topographic mapping was assessed by measuring the distance between the tips of temporal and nasal axons and the isthmus (X and Y values, see Figure 2A). For each sample, the three posterior-most extending temporal axons and the three most posterior projecting nasal axons were measured (six axons per brain) and averaged respectively. These two average values were used to calculate the X/Y ratio. Data represent pooled results from at least three independent experiments. Statistical analyses were performed using Kruskal-Wallis test in the Instat software (GraphPad).

For quantitation of extracellular Engrailed immunostaining, tecta were flat mounted (dorsal side up), images were captured using the same gain settings, and care was taken to avoid pixel saturation. A rectangle was drawn from the posterior tectal boundary (isthmus) to the anterior tectum, positioned in the middle of the tectum (calculated using the D-V extent of the isthmus; Figure 2C), and pixel intensity per unit area was calculated with ImageJ (1.38×). Pixel intensity profiles were plotted along the A-P axis of the rectangle, and the anterior/posterior ratios were calculated. To compensate for size variations between samples, images were normalized using the tectal borders.

Statistics

Tests and significance are indicated in figure legends; all error bars represent SEM unless otherwise specified.

SUPPLEMENTAL DATA

Supplemental Data include Supplemental Experimental Procedures, Supplemental Discussions, and six figures and can be found with this article online at http://www.cell.com/neuron/supplemental/S0896-6273(09)00718-1.

ACKNOWLEDGMENTS

We thank Drs. William Harris, Kenneth Moya, and Michel Volovitch for useful discussions. We are indebted to Raoul Torero-Ibad for En1/2 production, to Louis Leung for his blind analyses of turning assay results, and to Julien Falk, Kimmy Leung, Patricia Jusuf, and Hosung Jung for image analysis. Dr. Sophie Layalle provided a protocol to visualize extracellular proteins in *Xenopus* embryos. This work was supported by Agence Nationale de la Recherche (ANR06, Neuro-013-01), a Wellcome Trust Programme Grant (WT070568 & WT085314), the Deutsche Forschungsgemeinschaft (Förderkennzeichen WU164/4-1; WU164/3-2) and the EU-project HPRN-CT-2001-00242. I.B. was financed by Fondation pour la Recherche Médicale (FDT20061209092).

Accepted: September 4, 2009
Published: November 11, 2009

REFERENCES

Auerbach, R., Kubai, L., Knighton, D., and Folkman, J. (1974). A simple procedure for the long-term cultivation of chicken embryos. Dev. Biol. *41*, 391–394.

Auf der Maur, A., Tissot, K., and Barberis, A. (2004). Antigen-independent selection of intracellular stable antibody frameworks. Methods *34*, 215–224.

Bovolenta, P. (2005). Morphogen signaling at the vertebrate growth cone: a few cases or a general strategy? J. Neurobiol. *64*, 405–416.

Brunet, I., Weinl, C., Piper, M., Trembleau, A., Volovitch, M., Harris, W., Prochiantz, A., and Holt, C. (2005). The transcription factor Engrailed-2 guides retinal axons. Nature *438*, 94–98.

Brunet, I., Di Nardo, A.A., Sonnier, L., Beurdeley, M., and Prochiantz, A. (2007). The topological role of homeoproteins in the developing central nervous system. Trends Neurosci. *30*, 260–267.

Buhusi, M., Schlatter, M.C., Demyanenko, G.P., Thresher, R., and Maness, P.F. (2008). L1 interaction with ankyrin regulates mediolateral topography in the retinocollicular projection. J. Neurosci. *28*, 177–188.

Cheng, H.J., Nakamoto, M., Bergemann, A.D., and Flanagan, J.G. (1995). Complementary gradients in expression and binding of ELF-1 and Mek4 in development of the topographic retinotectal projection map. Cell *82*, 371–381.

Chien, C.B., Rosenthal, D.E., Harris, W.A., and Holt, C.E. (1993). Navigational errors made by growth cones without filopodia in the embryonic Xenopus brain. Neuron *11*, 237–251.

Ciossek, T., Monschau, B., Kremoser, C., Loschinger, J., Lang, S., Muller, B.K., Bonhoeffer, F., and Drescher, U. (1998). Eph receptor-ligand interactions are necessary for guidance of retinal ganglion cell axons in vitro. Eur. J. Neurosci. *10*, 1574–1580.

Claudepierre, T., Koncina, E., Pfrieger, F.W., Bagnard, D., Aunis, D., and Reber, M. (2008). Implication of neuropilin 2/semaphorin 3F in retinocollicular map formation. Dev. Dyn. *237*, 3394–3403.

Di Nardo, A.A., Nedelec, S., Trembleau, A., Volovitch, M., Prochiantz, A., and Montesinos, M.L. (2007). Dendritic localization and activity-dependent translation of Engrailed1 transcription factor. Mol. Cell. Neurosci. *35*, 230–236.

Drescher, U., Kremoser, C., Handwerker, C., Loschinger, J., Noda, M., and Bonhoeffer, F. (1995). In vitro guidance of retinal ganglion cell axons by RAGS, a 25 kDa tectal protein related to ligands for Eph receptor tyrosine kinases. Cell *82*, 359–370.

Dutting, D., and Meyer, S.U. (1995). Transplantations of the chick eye anlage reveal an early determination of nasotemporal polarity. Int. J. Dev. Biol. *39*, 921–931.

Falk, J., Drinjakovic, J., Leung, K.M., Dwivedy, A., Regan, A.G., Piper, M., and Holt, C.E. (2007). Electroporation of cDNA/Morpholinos to targeted areas of embryonic CNS in Xenopus. BMC Dev. Biol. *7*, 107.

Feldheim, D.A., Kim, Y.I., Bergemann, A.D., Frisen, J., Barbacid, M., and Flanagan, J.G. (2000). Genetic analysis of ephrin-A2 and ephrin-A5 shows their requirement in multiple aspects of retinocollicular mapping. Neuron *25*, 563–574.

Feldheim, D.A., Nakamoto, M., Osterfield, M., Gale, N.W., DeChiara, T.M., Rohatgi, R., Yancopoulos, G.D., and Flanagan, J.G. (2004). Loss-of-function analysis of EphA receptors in retinotectal mapping. J. Neurosci. *24*, 2542–2550.

Flanagan, J.G. (2006). Neural map specification by gradients. Curr. Opin. Neurobiol. *16*, 59–66.

Friedman, G.C., and O'Leary, D.D. (1996). Retroviral misexpression of engrailed genes in the chick optic tectum perturbs the topographic targeting of retinal axons. J. Neurosci. *16*, 5498–5509.

Frisen, J., Yates, P.A., McLaughlin, T., Friedman, G.C., O'Leary, D.D., and Barbacid, M. (1998). Ephrin-A5 (AL-1/RAGS) is essential for proper retinal axon guidance and topographic mapping in the mammalian visual system. Neuron *20*, 235–243.

Furrer, M.P., Vasenkova, I., Kamiyama, D., Rosado, Y., and Chiba, A. (2007). Slit and Robo control the development of dendrites in Drosophila CNS. Development *134*, 3795–3804.

Gingras, A.C., Raught, B., and Sonenberg, N. (1999). eIF4 initiation factors: effectors of mRNA recruitment to ribosomes and regulators of translation. Annu. Rev. Biochem. *68*, 913–963.

Haas, K., Sin, W.C., Javaherian, A., Li, Z., and Cline, H.T. (2001). Single-cell electroporation for gene transfer in vivo. Neuron *29*, 583–591.

Hanks, M., Wurst, W., Anson-Cartwright, L., Auerbach, A.B., and Joyner, A.L. (1995). Rescue of the En-1 mutant phenotype by replacement of En-1 with En-2. Science *269*, 679–682.

Hansen, M.J., Dallal, G.E., and Flanagan, J.G. (2004). Retinal axon response to ephrin-as shows a graded, concentration-dependent transition from growth promotion to inhibition. Neuron *42*, 717–730.

Hemmati-Brivanlou, A., de la Torre, J.R., Holt, C., and Harland, R.M. (1991). Cephalic expression and molecular characterization of Xenopus En-2. Development *111*, 715–724.

Holcman, D., Kasatkin, V., and Prochiantz, A. (2007). Modeling homeoprotein intercellular transfer unveils a parsimonious mechanism for gradient and boundary formation in early brain development. J. Theor. Biol. *249*, 503–517.

Hornberger, M.R., Dutting, D., Ciossek, T., Yamada, T., Handwerker, C., Lang, S., Weth, F., Huf, J., Wessel, R., Logan, C., et al. (1999). Modulation of EphA receptor function by coexpressed ephrinA ligands on retinal ganglion cell axons. Neuron *22*, 731–742.

Itasaki, N., and Nakamura, H. (1996). A role for gradient en expression in positional specification on the optic tectum. Neuron *16*, 55–62.

Joliot, A., and Prochiantz, A. (2004). Transduction peptides: from technology to physiology. Nat. Cell Biol. *6*, 189–196.

Joliot, A., Trembleau, A., Raposo, G., Calvet, S., Volovitch, M., and Prochiantz, A. (1997). Association of Engrailed homeoproteins with vesicles presenting caveolae-like properties. Development *124*, 1865–1875.

Joyner, A.L., and Hanks, M. (1991). The engrailed genes: evolution and function. Seminar in Developmental Biology 2, 736–741.

Knoll, B., Weinl, C., Nordheim, A., and Bonhoeffer, F. (2007). Stripe assay to examine axonal guidance and cell migration. Nat. Protocols *2*, 1216–1224.

Lesaffre, B., Joliot, A., Prochiantz, A., and Volovitch, M. (2007). Direct non-cell autonomous Pax6 activity regulates eye development in the zebrafish. Neural Develop. *2*, 2.

Logan, C., Wizenmann, A., Drescher, U., Monschau, B., Bonhoeffer, F., and Lumsden, A. (1996). Rostral optic tectum acquires caudal characteristics following ectopic engrailed expression. Curr. Biol. *6*, 1006–1014.

Mann, F., Ray, S., Harris, W., and Holt, C. (2002). Topographic mapping in dorsoventral axis of the Xenopus retinotectal system depends on signaling through ephrin-B ligands. Neuron *35*, 461–473.

McFarlane, S., Cornel, E., Amaya, E., and Holt, C.E. (1996). Inhibition of FGF receptor activity in retinal ganglion cell axons causes errors in target recognition. Neuron *17*, 245–254.

McLaughlin, T., and O'Leary, D.D. (2005). Molecular gradients and development of retinotopic maps. Annu. Rev. Neurosci. *28*, 327–355.

Mueller, B.K., Dutting, D., Haase, A., Feucht, A., and Macchi, P. (1998). Partial respecification of nasotemporal polarity in double-temporal chick and chimeric chick-quail eyes. Mech. Dev. *74*, 15–28.

Nakamura, N., Lowe, M., Levine, T.P., Rabouille, C., and Warren, G. (1997). The vesicle docking protein p115 binds GM130, a cis-Golgi matrix protein, in a mitotically regulated manner. Cell *89*, 445–455.

O'Leary, D.D., and Nakagawa, Y. (2002). Patterning centers, regulatory genes and extrinsic mechanisms controlling arealization of the neocortex. Curr. Opin. Neurobiol. *12*, 14–25.

O'Leary, D.D., and McLaughlin, T. (2005). Mechanisms of retinotopic map development: Ephs, ephrins, and spontaneous correlated retinal activity. Prog. Brain Res. *147*, 43–65.

Pfeiffenberger, C., Yamada, J., and Feldheim, D.A. (2006). Ephrin-As and patterned retinal activity act together in the development of topographic maps in the primary visual system. J. Neurosci. *26*, 12873–12884.

Raper, J.A., and Kapfhammer, J.P. (1990). The enrichment of a neuronal growth cone collapsing activity from embryonic chick brain. Neuron *4*, 21–29.

Sakaguchi, D.S., Moeller, J.F., Coffman, C.R., Gallenson, N., and Harris, W.A. (1989). Growth cone interactions with a glial cell line from embryonic Xenopus retina. Dev. Biol. *134*, 158–174.

Schmid, R.S., and Maness, P.F. (2008). L1 and NCAM adhesion molecules as signaling coreceptors in neuronal migration and process outgrowth. Curr. Opin. Neurobiol. *18*, 245–250.

Shigetani, Y., Funahashi, J.I., and Nakamura, H. (1997). En-2 regulates the expression of the ligands for Eph type tyrosine kinases in chick embryonic tectum. Neurosci. Res. *27*, 211–217.

Sonnier, L., Le Pen, G., Hartmann, A., Bizot, J.C., Trovero, F., Krebs, M.O., and Prochiantz, A. (2007). Progressive loss of dopaminergic neurons in the ventral midbrain of adult mice heterozygote for Engrailed1. J. Neurosci. *27*, 1063–1071.

Sperry, R.W. (1963). Chemoaffinity in the orderly growth of nerve fiber patterns and connections. Proc. Natl. Acad. Sci. USA *50*, 703–710.

Strochlic, L., Dwivedy, A., van Horck, F.P., Falk, J., and Holt, C.E. (2008). A role for S1P signalling in axon guidance in the Xenopus visual system. Development *135*, 333–342.

Strube, R.W., and Chen, S.Y. (2004). Enhanced intracellular stability of sFv-Fc fusion intrabodies. Methods *34*, 179–183.

Sugiyama, S., Di Nardo, A.A., Aizawa, S., Matsuo, I., Volovitch, M., Prochiantz, A., and Hensch, T.K. (2008). Experience-dependent transfer of Otx2 homeoprotein into the visual cortex activates postnatal plasticity. Cell *134*, 508–520.

Swartz, M., Eberhart, J., Mastick, G.S., and Krull, C.E. (2001). Sparking new frontiers: using in vivo electroporation for genetic manipulations. Dev. Biol. *233*, 13–21.

Thanos, S. (1991). Specific transcellular carbocyanine-labelling of rat retinal microglia during injury-induced neuronal degeneration. Neurosci. Lett. *127*, 108–112.

Vielmetter, J., Stolze, B., Bonhoeffer, F., and Stuermer, C.A. (1990). In vitro assay to test differential substrate affinities of growing axons and migratory cells. Exp. Brain Res. *81*, 283–287.

Walter, J., Henke-Fahle, S., and Bonhoeffer, F. (1987a). Avoidance of posterior tectal membranes by temporal retinal axons. Development *101*, 909–913.

Walter, J., Kern-Veits, B., Huf, J., Stolze, B., and Bonhoeffer, F. (1987b). Recognition of position-specific properties of tectal cell membranes by retinal axons in vitro. Development *101*, 685–696.

Weinl, C., Becker, N., and Loeschinger, J. (2005). Responses of temporal retinal growth cones to ephrinA5-coated beads. J. Neurobiol. *62*, 219–230.

Wilkinson, D.G., and Nieto, M.A. (1993). Detection of messenger RNA by in situ hybridization to tissue sections and whole mounts. Methods Enzymol. *225*, 361–373.

Wurst, W., Auerbach, A.B., and Joyner, A.L. (1994). Multiple developmental defects in Engrailed-1 mutant mice: an early mid- hindbrain deletion and patterning defects in forelimbs and sternum. Development *120*, 2065–2075.

Yates, P.A., Roskies, A.L., McLaughlin, T., and O'Leary, D.D. (2001). Topographic-specific axon branching controlled by ephrin-As is the critical event in retinotectal map development. J. Neurosci. *21*, 8548–8563.